Catalytic Properties of Bimetallic Catalysts Based on Binary Complexes of Transition Metals in Fischer–Tropsch Synthesis

A. A. KHASSIN[1], S. I. PECHENYUK[2], D. P. DOMONOV[2], T. P. MINYUKOVA, G. K. CHERMASHENTSEVA[1], G. N. KUSTOVA[1] and L. M. PLYASOVA[1]

[1]*Boreskov Institute of Catalysis, Siberian Branch of the Russian Academy of Sciences, Pr. Akademika Lavrentyeva 5, Novosibirsk 630090 (Russia)*

E-mail: aakhassin@catalysis.ru

[2]*Tananaev Institute of Chemistry and Technology of Rare Elements and Mineral Raw Materials, Kola Science Centre of the Russian Academy of Sciences, Ul. Fersmana 26A, Apatity184209 (Russia)*

(Received October 19, 2006; revised October 24, 2007)

Abstract

The possibility to prepare bimetallic catalysts Fe–Ni, Fe–Co and Co–Cu through thermolysis of binary complex salts involving a complex cation of one metal and a complex anion of other one is discussed, and their catalytic properties in Fischer–Tropsch synthesis are presented. Our study revealed that deposition of binary complex salts having composition $[Ni(NH_3)_6]_3[Fe(CN)_6]_2$, $[Co(NH_3)_6][Fe(CN)_6]$ and $[Co(NH_3)_6]_2C_2O_4[Cu(C_2O_4)_2]_2$ on to the surface of aluminium hydroxide and subsequent thermolysis of the obtained composition give the chance to have metallic particles of size 15–40 nm fixed on the surface of aluminium oxide. In the case of binary complexes Ni–Fe and Co–Fe, the formation of bimetallic particles of size 15–16 nm and respective structures FCC and BCC is observed. Break-up of complexes proceeds in several sequential exothermic stages. The catalytic properties of bimetallic particles Fe–Co of BCC structure, which are prepared by thermolysis of $[Co(NH_3)_6][Fe(CN)_6]$ + $Al(OH)_3$ composition, differ essentially from the literature data for Co–Fe catalysts by the reduced activity of the prepared particles with respect to the secondary processes for hydrogenation of olefins. This feature manifests itself in the extremely high selectivity of the process in relation to olefines and its anomalous temperature dependence. A rise in the process pressure up to 10–20 atm leads to significant changes in catalytic properties of bimetallic Co–Fe catalysts, among them the loss of selectivity in relation to olefins and the decrease in the rate of secondary process of vapour conversion of CO. The pressure dependence of process passing character is caused by variation in structure of catalytically active component under the action of reagents.

INTRODUCTION

Preparation of synthetic motor fuels and raw materials for chemical industry from alternative sources is an actual problem, and its effective solution is liable to determine in many respects the stability of evolution in the immediate future. Process for conversion of CO–H_2 mixture (synthesis gas) into hydrocarbons, which proceeds in the presence of catalysts containing metals of Group VIII (Fischer–Tropsch synthesis, FTS), remains for the present unique in having advantageous use in practice for this purpose [1]. Iron and cobalt are constituents of commercial catalysts of this synthesis. Among FTS products, hydrocarbons with a number of carbon atoms more than 5 (fraction C_{5+}) and α-olefins, which can be used as valuable chemical raw materials, are of most value. Selectivity of synthesis is described by α-parameter in an equation of so-called Anderson–Schulz–Flory (ASF) distribution:

$M_n = (1 - \alpha)\alpha^{n-1}$; $W_n = (1 - \alpha)^2 n\alpha^{n-1}$

where M_n and W_n are molar and mass portions of hydrocarbons involving n carbon atoms in carbon chain [2, 3].

Catalytic properties in FTS are determined by character of active component particles [4] and their size [5, 6]. As noted in series of recent papers [7, 8], bimetallic catalysts based on Fe–Co are of pronounced selectivity with

respect to α-olefines and appear to have considerable promise for use in synthesis of hydrocarbons that is oriented to producing a valuable chemical starting material. The possibility to prepare bimetallic catalysts Fe–Ni, Fe–Co, and Co–Cu through thermolysis of binary complex salts and their catalytic properties in FTS are investigated in our work. It may be suggested that metallic phase derived from binary complex decomposition is to present bimetallic particles of high dispersity. Catalytic properties of bimetallic particles of this sort can essentially differ from catalytic properties of individual metals or their mechanical mixtures.

EXPERIMENTAL

The previously obtained data [9, 10] have shown that thermolysis of binary complex salts without their adsorption on oxide support gives rise to metallic particles of micrometric size. It is known at the same time that the optimal size of particles for highly active cobalt- and nickel-containing catalysts is only 6–8 nm [11].

Binary complex salts containing complex cations $[Co(NH_3)_6]^{3+}$ and $[Ni(NH_3)_6]^{2+}$ and complex anions $[Fe(CN)_6]^{3-}$ and $[Cu(C_2O_4)_2]^{2-}$ were used for producing bimetallic catalysts. Complexes were prepared by the procedures described in [12, 13]. Cobalt (II) carbonate, sodium oxalate, copper sulphate, a concentrated solution of ammonia, and reactive potassium ferricyanide $K_3[Fe(CN)_6]$ were used as initial materials for synthesis. All initial materials were analytically pure. Complexes $[Co(NH_3)_6]Cl_3$, $[Ni(NH_3)_6]Cl_2$, and $Na_2[Cu(C_2O_4)_2]$ were synthesized as in [14, 15]. The precipitation of binary complex salts was performed from concentrated solutions of starting complexes taken in stoichiometric proportion of the planned composition. The element analysis data for prepared binary complex salts are tabulated in Table 1. Control over the purity of salt deposition was also carried out with the help of IR spectroscopy and X-ray analysis.

Four techniques for fixing binary salt to the supporter were used (Series 1–1V).

Series 1 was prepared by impregnation of porous supporter (BAC, γ-Al_2O_3) with solution of salt, whereas Series II was prepared by mixing of binary complex salt with the suspension containing aluminium hydroxide that transformed to oxide in the course of subsequent heat treatment of obtained composition. The data on the content of metals in obtained samples are tabulated in Table 2.

Standard commercial carbon BAC (S = 438 m^2/g) and granulated γ-Al_2O_3 (S = 133 m^2/g) were used as supporters for preparation of samples by impregnation procedure. The specific moisture capacity of supporter was found experimentally, and this parameter was used in repeated impregnation of supporter by saturated solution of cation complex with drying in the air after each impregnation. Thereafter supporter was impregnated by saturated solution of complex anion with the use of analogous strategy.

The serie III and IV were concerned with deposition of binary salt in pore space of supporter and were aimed at decreasing the size of bimetallic particles generated at the stage of reducing activation. The series III was prepared by consecutive impregnation of silica gels of different porous structure by solutions of monocomplex salts containing cation and anion of binary salt. The following silica gels were used: KCK-2 with specific surface 420 m^2/g, KCC-3 (540 m^2/g), KCC (220 m^2/g), KCM-6 (600 m^2/g), and KCMG (450 m^2/g). As the ex-

TABLE 1

Data on element analysis of binary complex salts used for preparation of bimetallic catalysts

Complex	Content, mass %		
	Metal 1	Metal 2	Carbon
$[Co(NH_3)_6][Fe(CN)_6]$	Co, 15.8/16.2	Fe, 15.0/15.1	19.3/19.3
$[Ni(NH_3)_6]_3[Fe(CN)_6]_2$	Ni, 19.4/20.3	Fe, 12.3/13.1	–/–
$[Co(NH_3)_6]_2C_2O_4[Cu(C_2O_4)_2]_2 \cdot 2H_2O$	Co, 12.7/12.4	Cu, 14.3/14.3	13.5/13.2

Note. First value is calculated, second one is found.

TABLE 2

Data on chemical composition of starting samples of bimetallic catalysts based on binary complex salts in series I and II

Sample	Complex	Supporter	Content, mass %		Moisture, %	Mode
			Metal 1	Metal 2		of preparation
I-1	$[Co(NH_3)_6][Fe(CN)_6]$	БАУ	Co, 2.33	Fe, 1.92	10	Impregnation
I-2	$[Co(NH_3)_6]_2C_2O_4[Cu(C_2O_4)_2]_2$	БАУ	Co, 2.64	Cu, 1.54	12	»
I-4	$[Ni(NH_3)_6]_3[Fe(CN)_6]_2$	БАУ	Ni, 0.89	Fe, 0.86	16	»
I-5	$[Co(NH_3)_6][Fe(CN)_6]$	γ-Al_2O_3	Co, 0.80	Fe, 0.78	10	»
II-1	$[Ni(NH_3)_6]_3[Fe(CN)_6]_2$	$Al(OH)_3$	Ni, 6.23	Fe, 3.88	–	Mixing
II-2	$[Co(NH_3)_6][Fe(CN)_6]$	$Al(OH)_3$	Co, 5.14	Fe, 4.97	–	»
II-3	$[Co(NH_3)_6]_2C_2O_4[Cu(C_2O_4)_2]_2$	$Al(OH)_3$	Co, 4.84	Cu, 5.40	–	»

periments have shown, the binary salt is formed owing to $K_3[Fe(CN)_6] + [Co(NH_3)_6]Cl_3$ impregnation, however this salt is not fixed in pore space of supporter after the first impregnation because of $[Fe(CN)_6]^{3-}$ anion polymerisation. The impregnation experiments in an orderly sequence $[Co(NH_3)_6]Cl_3 + K_3[Fe(CN)_6]$ were more advantageous, however the amount of fixed metals was only insignificant. Samples CoFeIII-7 and CoFeIII-8 were selected for testing (Table 3).

The series IV was prepared by precipitating binary salt in the presence of $Al(OH)_3$ suspension. The element analysis data for starting composition and a percentage of metals in reduced samples are presented in Table 4.

TABLE 3

Percentage of metal cations in samples of CoFeIII series

Sample	Supporter	Content, mass %		Co : Fe
		Co	Fe	
CoFeIII-7	KCMG	0.28	0.07	3.8
CoFeIII-8	KCC	0.96	0.7	1.3

Infrared spectra were recorded in the range 350–4000 cm^{-1} using a Bomem MB-102 infrared spectrometer. The powdered catalysts were introduced in KBr matrix.

X-ray diffraction investigations were carried out with the use of Siemens D-500 and Bruker D-8 (CuK_α emission) diffractometers, and β-lines were removed from the reflected beam by graphite monochromator. For calcined and reduced samples, the measurements were performed near immediately after their extraction into the air.

The catalytic properties were studied in flow tube reactor with stationary grain layer of catalyst at a pressure from 1 to 20.8 atm and at 210–290 °C. The composition of reaction mixture at entry into the reactor was kept in the proportion $CO : H_2 : N_2 = 3 : 6 : 1$ (nitrogen was used as an inner standard). A charge of 1.8–2.5 g of catalyst grains of size 0.14–0.25 mm was mixed with quartz in the 1 : 1 ratio. Reaction products were analysed by chromatographic method in steam-gas phase and in the phases of liquid products condensed at 20 °C as well as extracted with *n*-hexane from catalyst after catalytic experiments.

TABLE 4

Data on Co and Fe content in catalyst samples of CoFeIV series

Sample	Content in starting composition, mass %			Mass loss on activation, %	Co + Fe content in reduced catalyst, mass %
	Co	Fe	Water		
CoFeIV-1	1.93	1.83	26.6	35.1	5.8
CoFeIV-2	3.67	3.48	25.4	41.6	12.3
CoFeIV-3	7.08	6.72	16.4	47.7	26.4

RESULTS AND DISCUSSION

Evolution of "binary complex salt + supporter" compositions in the course of the thermolysis

The infrared spectra of the samples of catalysts precursors have made it possible to obtain evidence on the state of metal cations in them. Thus for composition CoFeII-1 ($[Co(NH_3)_6][Fe(CN)_6]$ and $Al(OH)_3$) (Fig. 1, curve *2*) an intense band at 2114 cm^{-1} closely approximating that of F_{1u} oscillations of complex anion $[Fe(CN)_6]^{3-}$ and absorption bands of complex cation $[Co(NH_3)_6]^{3+}$ at 1328, 1623 and 839 cm^{-1} are observed in the spectrum, suggesting that the initial complex is present in the composition. An intense band at 1384 cm^{-1} and weak bands at 1763 and 826 cm^{-1} are to be related to NO_3^- anion whose presence in the sample is apparently associated with the use of aluminium nitrate solution for precipitating hydroxide $Al(OH)_3$. The intensity of Co^{3+} ammonium complex bands is moderate, however the band at 1384 cm^{-1} has a marked "arm" at ~1410 cm^{-1} that corresponds to NH_4^+ oscillations. A distinct absorption in the region 2020–2090 cm^{-1} can be associated with complex anion $[Fe(CN)_6]^{4-}$ containing Fe(II). The presence of these groups in the composition of the sample points to some interaction of complex with aluminium hydroxide that is followed by Fe^{3+} reduction and NH_4^+ formation. It is necessary to note that the presence of NH_4^+ cation in the sample composition can be associated with inadequate washing aluminium hydroxide of ammonium nitrate after precipitation. Spectrum of $[Co(NH_3)_6][Fe(CN)_6]$ + γ-Al_2O_3 sample is akin to that discussed above.

Suddenly quite another structure of spectrum is observed for $[Co(NH_3)_6][Fe(CN)_6]$/BAC sample. The intensity of the band at 1328 cm^{-1} is small, whereas a very intense absorption is observed at 1409 cm^{-1}, suggesting that a high degree of conversion of NH_3 ligands into NH_4^+ ions takes place. The bands 2114 and 2027 cm^{-1}, which are evidently related to Fe^{3+} and Fe^{2+} cyanide complexes respectively, are silhouetted against the background of the intense wide band having a maximum at ~2080 cm^{-1} that fits the valence oscillation of $[Fe^{3+}(CN)_5]^{2-}$ complex of the symmetry reduced to C_{4x} or $[Fe^{2+}(CN)_5]^{3-}$ complex what is more probable.

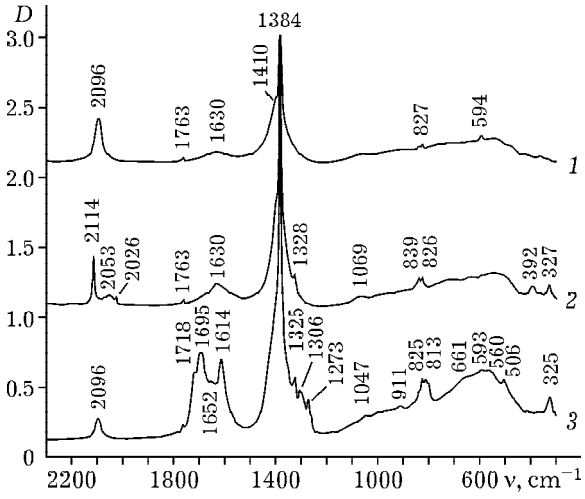

Fig. 1. Absorption spectra of samples: *1* – NiFeII-1, composition $[Ni(NH_3)_6]_3[Fe(CN)_6]_2$ + $Al(OH)_3$, *2* – CoFeII-2, $[Co(NH_3)_6][Fe(CN)_6]$ + $Al(OH)_3$, *3* – CoCuII-3, $[Co(NH_3)_6]_2C_2O_4[Cu(C_2O_4)_2]_2$ + $Al(OH)_3$.

In such an event, the absorption observed at 590 cm^{-1} falls to deformation oscillation of this complex. We should note that this sample has also a sizable proportion of nitrate ions (absorption at 1385 cm^{-1}). However the obtained data are inadequate to discuss the mechanism of the interaction of $[Co(NH_3)_6][Fe(CN)_6]$ binary complex with BAC surface.

Spectra of the samples prepared by deposition of Fe–Ni complex $[Ni(NH_3)_6]_3[Fe(CN)_6]_2$ on BAC and aluminium hydroxide testify that the binary complex has been completely decomposed. Thus for $[Ni(NH_3)_6]_3[Fe(CN)_6]_2$/BAC sample the band 1328 cm^{-1} of hexamine complex cation is completely absent, whereas the intense band at 1410 cm^{-1} points to the formation of NH_4^+ cations. In the regions of Fe–C–N oscillations an uniform intense band (2094 cm^{-1}) and a weak band (594 cm^{-1}) are observed, which can be assigned to $[Fe^{3+}(CN)_5]^{2-}$ anion. It is possible that this process is due to interaction with a supporter, although ammonia, as noted in [13], is partially liberated even from unsupported binary complex salt with the formation of the green deposit. Spectrum of NiFeII-1 composition differs from the discussed one only by the presence of a very intense band at 1384 cm^{-1} and weak bands at 1763 and 827 cm^{-1} appropriate to NO_3^- anion.

The group of absorption bands at 1719, 1695, 1652, and 1614 cm^{-1} as well as the bands

at 1273 and 813 cm^{-1} observed for CoCuII-3 sample refer to $[Cu(C_2O_4)_2]^{2-}$ anion. The absorption at 1325 cm^{-1} corresponds to oscillations of NH_3 ligand of a complex cation. However the availability of spectral bands at 2096 and 594 cm^{-1}, which are lacking in the unsupported binary complex spectrum, points to a partial decomposition of complex with the formation of CN groups. We should note that the inverse process of the formation of oxalate and ammonium ions in oxidizing CN groups under the action of peroxocomplexes was hitherto observed (for one example, see [16]). The sample of CoCuII-3 composition, as well as the samples discussed above, contains NO_3^- anions.

The thermolysis of samples of the supported complexes in the inert and reducing atmosphere was studied with the use of a Netzsch STA-409 system of thermogravimetric analysis in circumstances when a rise in sample temperature was equal to 3 K/min. The data of thermal analysis point to the highly exothermic decomposition of complexes at temperatures in excess of 160 °C (compositions containing Ni–Fe complexes), 180° (Co–Fe) or 230 °C (compositions with Co–Cu complex). On ignition in argon stream at the rate of temperature rise 3 K/min, the explosive one-step decomposition takes place with crucible overheating by 20–30 K. Because of this, the following measurements were carried out at the rate of temperature rise 0.5 K/min (in argon stream) and 1 K/min (in hydrogen stream). These investigations have revealed a complicated character of processes proceeding in several consecutive stages.

To take an illustration, the basic effect of NiFeII-1 sample decomposition is observed in both cases (in Ar and in H_2) at 170–190 °C (a highly exothermic effect), and the mass losses about 37 % (in argon) and 31 % (in hydrogen) are noted (Fig. 2). An additional loss of initial mass (8–9 %) takes place at 210–230 °C. A further exothermic effect of the mass loss (~10 mass %) is observed at 290–300 °C. Two weak endothermic effects at 440 and 640 °C are apparently connected with the following ignition of aluminium oxide (the sum of mass losses is 2–3 %). At not too low temperatures (below 150 °C) the sample drying with mass loss in the region of 7–9 % is at work. The total mass loss is over 60 %, and 40–45 % in this case correspond to a temperature interval stretching from 160 to 250 °C where the thermolysis of the complex takes place.

The data of thermogravimetry allow us to propose that the formation of metallic particles, which can show a catalytic activity in hydrogenation processes, is due to thermolysis. However *ex situ* investigation of the samples after thermolysis is associated with their extraction in midair, which is why a good passivation of the surface of metallic phase is required after activation. The passivation of this sort can be carried out during conditions of the reaction of CO hydrogenation that is accompanied by stabilizing C_xH_y intermediates at the surface of metallic phase. Because of this, a phase constitution was investigated for the samples as were up to then used for catalytic tests.

The results of X-ray diffraction are presented in Fig. 3. The sample $[Co(NH_3)_6][Fe(CN)_6]$ + $Al(OH)_3$, upon activation in a temperature-programmed regime up to 380 °C, shows X-ray diffraction lines for d equal to 2.02 and 1.42 Å, which fit the diffraction by (110) and (200) planes of the metal having a body-centred cubic lattice that is characteristic of Fe^0. The lattice parameter a_{Fe} of Fe^0 phase is equal to 2.866 Å (JCPDS file 06-0696), which far exceeds our value 2.852 Å and can point to the formation of Fe–Co intermetallic compound having a bcc structure. Notice that the forma-

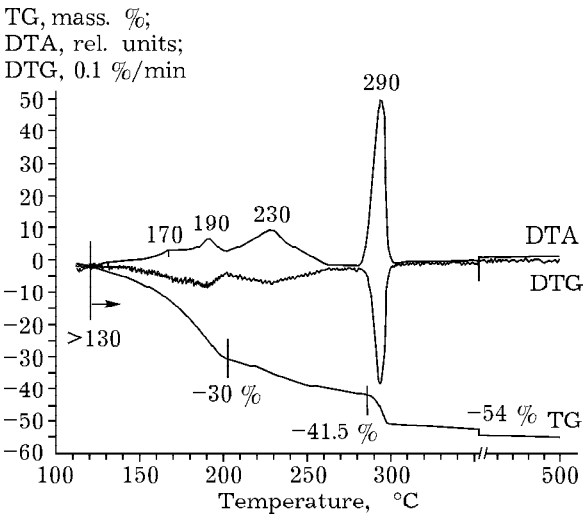

Fig. 2. Thermogravimetry of the sample $Ni(NH_3)_6]_3[Fe(CN)_6]_2$ + $Al(OH)_3$ in hydrogen stream. The rate of temperature rise between 120–200 °C is 1 K/min and 3 K/min between 200–500 °C.

tion of this structure, according to a large body of literature data (to illustrate, see [17, 18]), is typical for Co–Fe intermetallic compounds. Analysis of EXAFS data [19] makes it possible to propose that the surface of Co–Fe intermetallic compounds is enriched in Fe, whereas Co atoms are localized for the most part in the particle bulk. By line width (see Fig. 3, curve *1*), the average size of the coherent scattering region, that is, the size of metal particles, can be estimated; it is equal to 16 nm. The phases having fcc and hexagonal close packings, which are typical for metallic cobalt, have not found in the sample.

The data of X-ray diffraction of $[Ni(NH_3)_6]_3[Fe(CN)_6]_2 + Al(OH)_3$ sample after thermolysis with the top temperature 320 °C can also be explained as a formation of Ni–Fe bimetallic particles while having fcc structure that is typical for metallic nickel. The lines at 2.06, 1.79 and 1.42 relate to fcc structure of metallic particles. A wide halo at 2.42 (area 36°) supposedly relates to NiO dispersed particles. The characteristic size of particles determined from the width of diffraction lines comprises 15 nm.

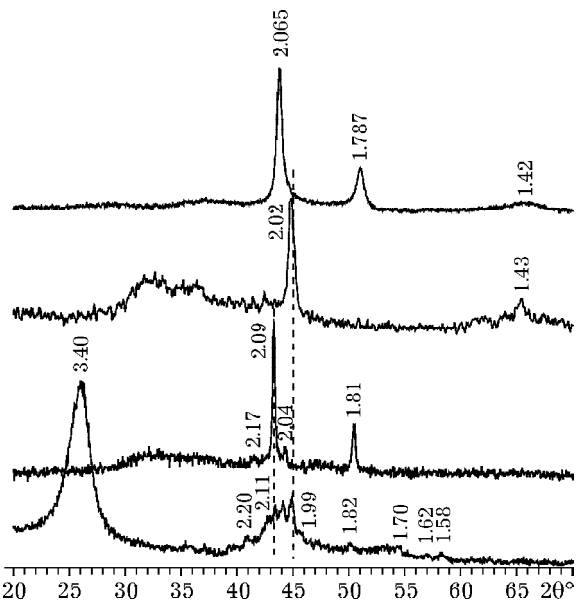

Fig. 3. X-ray diffraction data for samples after thermolysis in hydrogen stream and catalytic experiments in Fischer–Tropsch synthesis at a pressure of 1 atm: *1* – NiFeII-1, $[Ni(NH_3)_6]_3[Fe(CN)_6]_2 + Al(OH)_3$, *2* – CoFeII-2, $[Co(NH_3)_6][Fe(CN)_6] + Al(OH)_3$, *3* – CoCuII-3, $[Co(NH_3)_6]_2C_2O_4[Cu(C_2O_4)_2]_2 + Al(OH)_3$, *4* – CoFeII-2 at a pressure of 20.8 atm.

Unlike Co–Fe and Ni–Fe complexes, the thermolysis of CoCuII-3 sample at 280 and 350 °C does not lead to the formation of bimetallic phase: diffraction lines of Cu^o particles at 2.09 and 1.81 Å and the lines at 2.17 and 2.04 Å, which relate to cobalt carbide Co_3C (JCPDS file 43-1144), are clearly shown on the roentgenogram. The formation of carbide phase in CO hydrogenation conditions at 1 atm is unlikely; this being so, it is most likely formed in the course of complex compound thermolysis as far as it goes. An oxalate ligand of Co^{2+} environment serves as a possible carbon source. The size of particles is about 39 nm for copper and under 20 nm for cobalt carbide.

Catalytic properties of catalysts in Fischer–Tropsch synthesis at a pressure of 1 atm

The results of testing samples of series II are tabulated in Table 5, and the results of testing Co–Fe catalysts of other series are tabulated in Table 6. In the latter case the dispersity of catalytically active component is lower in comparison with that in CoFeII-2 sample, which determines their low specific activity and lower selectivity.

The estimation of the noted catalytic activity related to one metal atom of metal surface has been carried out on the assumption of cuboctahedral form of particles. It will be recalled that the surface of Fe–Co bimetallic particles can be enriched in Fe [19]. The specific catalytic activity and parameter δ, which is representative of the selectivity of the sample containing particles of Ni–Fe alloy in respect to high molecular hydrocarbons, are correlated in magnitude with the corresponding characteristics of nickel-containing catalysts having similar-sized Ni particles, such as Ni/MgO catalysts [6]. However it is necessary to point out that the rate of secondary reaction of steam conversion of CO to CO_2 on the test sample is many times higher, resulting in a sizable proportion of CO_2 under reaction conditions. As this takes place, CO_2 portion grows with increasing temperature and degree of CO conversion. The water fraction that collects in the condenser arranged downstream of the reaction vessel contains a quantity of alcohols C_1–C_4 having a

molecular distribution following one of Anderson–Schulz–Flory with parameter $\alpha_{RO} = 0.27$.

The specific activity of the sample prepared by thermolysis of the composition $[Co(NH_3)_6][Fe(CN)_6] + Al(OH)_3$ is 2-3 times lower than it would be expected for monometallic cobalt catalysts containing particles of fcc cobalt of the same dispersity (see, for one, kinetic data [1] and data for Co/MgO catalysts [6]). The selectivity in respect of methane and parameter α for *n*-paraffins are somewhat below when compared to those for Co^0 particles of size 15 nm [20]. The content of olefins in reaction products is very high: C_3H_x products contain 87 % of propylene at 210 °C and more than 90 % at 250 °C, which far exceeds the corresponding values for Co- and even for Fe-containing catalysts. Notice that the extensive investigation of catalytic properties of bimetallic Fe–Co catalysts ($CoFe/TiO_2$ [18, 21, 22]) has not shown so high selectivity in respect of olefins. The fall of activity in secondary reactions of olefin conversion in the case of $CoFe/SiO_2$ catalysts, as compared with Co- and Fe-ones, was observed in [23], and here too the selectivity in respect of olefins was not so high. The reason why Fe–Co particles have reduced ability to activate olefins and hydrogenate a double bond C=C calls for further comprehensive investigation. The activity of the studied Fe–Co sample in reaction of steam conversion of CO is still higher compared to activity of Ni–Fe sample.

Parameter α for the fraction of olefins (0.52 at 210 °C and 0.46 at 250 °C) is also less as compared with that for Co^0 particles and yet much above than for the fraction of α-olefins: 0.32–0.26 (see Table 5). It may result from a predominance of β-olefins in C_{+5} products that appear to be formed from α-olefins at the surface of aluminium oxide.

It has been possible to perform analysis of the condensed products only for the most active samples (CoFeII-2 and CoFeI-5). Parameter α of ASF distribution in the condensed products was found to be higher compared to that for the fraction of products in gas phase (Table 7). Hence we have a distribution of products that is known in the literature as "twofold Flory" [24] and caused by the existence of two types of centres in the sample. These centres

TABLE 5

Results of catalytic tests of samples of series II in Fischer–Tropsch synthesis at a pressure of 1 atm

Parameter	NiFeII-1				CoFeII-2			CoCuII-3	
Content of Me(I) + Me(II), %	20				21			10.5	
Phase composition	Ni–Fe, fcc				Fe–Co, bcc			$Cu^0 + Co_3C$	
Particle size, nm	15				16			39	20
Estimate of number of surface centres Me^0, mmol/g_{cat}	0.27				0.28			0.11 (without Cu^0)	
Temperature, °C	210	230	250	210	230	250	210	230	250
Speed of gas flow, nL/(g_{cat} · h)	0.48	0.47	0.47	0.57	0.74	1.27	0.2	0.33	0.42
Degree of CO conversion, %	22.0	40.7	49.2	10.1	14.1	15.2	9.4	12.4	15.3
Rate of CO conversion, mmol/(g_{cat} · h)	1.4	2.6	3.1	0.65	1.4	2.7	0.21	0.54	0.87
Frequency of CO conversion, 10^{-3} s^{-1}	1.4	2.6	3.2	0.63	1.4	2.6	0.57	1.4	2.2
Noted E_{act} of CO conversion, kJ/mol	–				74			74	
Rate of CH_4 formation, μmol/(g_{cat} · h)	30	86	130	60	148	295	36	200	470
Frequency of centre in reaction of CO hydrogenation, 10^{-5} s^{-1}	3.1	8.7	13	5.8	14.5	29	9.2	50	120
Selectivity in respect of methane, % C	21	34	41	9.2	11	11	17	37	54
Noted E_{act} of methanation, kJ/mol	–				84			135	
Selectivity in respect of CO_2, % C	8.5	18	24	23	28	30	13	27	49
α_{ASF} for *n*-paraffins C_{3-7}	0.45	0.41	0.27	0.71	0.69	0.68	0.60	0.52	0.42
α_{ASF} for α-olefins C_{3-7}	0.32	0.29	0.28	0.32	0.29	0.26	0.58	0.40	0.37
C_3H_6/C_3H_8 ratio	0.41	0.28	0.24	6.0	6.9	10.2	0.9	0.85	0.64

TABLE 6

Results of catalytic tests of certain of the studied catalysts in Fischer–Tropsch synthesis at a pressure of 1 atm

Parameter	CoFeI-5			CoFeIII-8			CoFeIV-1	
	Procedure of preparation							
	Impregnation of γ-Al_2O_3 by Co–Fe complex colloid			Precipitation of Co–Fe in KCC pores			Precipitation of Co–Fe in $Al(OH)_3$ suspension	
Content of Me(1) + Me(2), mass %	6			2.3			5.8	
Phase composition	Fe–Co, bcc, γ-Al_2O_3			Fe–Co, bcc			Fe–Co, bcc, AlOOH	
Particle size, nm	16			25			40	
Number of surface centres Me^0, mmol/g_{cat}	0.08			0.035			0.03	
Temperature, °C	210	230	250	250	270	300	270	290
Speed of gas flow, nL/(g_{cat} · h)	0.11	0.18	0.35	0.11	0.11	0.11	0.1	0.1
Degree of CO conversion, %	12.5	15.5	13.8	5.6	11.6	22.6	5.8	18.7
Rate of CO conversion, mmol/(g_{cat} · h)	0.18	0.37	0.65	0.09	0.17	0.34	0.07	0.25
Frequency of CO conversion, $10^{-3}s^{-1}$	0.61	1.26	2.2	0.069	0.14	0.27	0.64	2.3
Noted E_{act} of CO conversion, kJ/mol	65			65			~100	
Rate of CH_4 formation, μmol/(g_{cat} · h)	19	43	94	15	27	42	12.5	33.2
Frequency of centre in reaction of CH_4 formation, 10^{-5} s^{-1}	6.4	14.6	32	12	22	34	11.6	31
Selectivity in respect of methane, % C	10.4	11.6	14.7	18	16	13	17	14
Noted E_{act} of methanation, kJ/mol	83			83			~84	
Selectivity in respect of CO_2, % C	17	14	23	17	19	17	32	17
α_{ASF} for *n*-paraffins C_{3-7}	0.62	0.62	0.70	0.61	0.63	0.61	0.66	0.48
α_{ASF} for α-olefins C_{3-7}	0.27	0.30	0.26	0.27	0.27	0.26	0.30	0.30
C_3H_6/C_3H_8 ratio	6.0	6.9	10.2	7.5	9.6	10.5	4.8	4.2

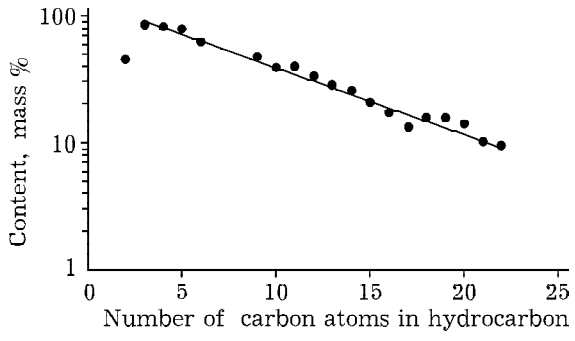

Fig. 4. Experimentally found content of olefins in reaction products against the number of carbon atoms for catalyst CoFeII-2 (T = 210 °C). Values for C_2–C_6 were obtained from analysis of gaseous hydrocarbons and from analysis of condensed products of reaction in the case of C_9–C_{22}.

are comparable in number and differ in the characteristic value of parameter α.

The content of olefins reduces also in accord with the exponential law

$(=/-)_n \sim \exp(-0.11n)$

as carbon atoms in molecule increase in number, confirming that parameter α for olefins is less as compared with this parameter for saturated hydrocarbons. However the content of olefins in products is reasonably high even for high molecular hydrocarbons (Fig. 4).

There is a need to note that χ-carbide of iron under reaction conditions is an active component of Fe-based monometallic catalysts, however the particles of carbide phase were not found in the constitution of Ni–Fe and Co–Fe samples.

TABLE 7

Results of analysis of the condensed products of Fischer–Tropsch synthesis

Sample	α		Olefin/paraffin ratio	
	n-paraffins	α-olefins	C_{10}	C_{18}
CoFeII-2	0.83	0.76	0.65	0.19
CoFeI-5	0.85	0.76	0.44	0.12

Catalytic properties of catalyst CoFeII-2 in Fischer–Tropsch synthesis at elevated pressures

The build-up of pressure (to 10.4 and 20.8 atm) tends to a marked increase in specific catalytic activity of catalysts with the noted overall order of a reaction ~1.1, whereas the order of relationship between the rate of methane formation (methanation route) and pressure is 1.3. These data are much above the ones characteristic of monometallic catalysts based on Co and Fe and comprising, by data [25] and [26], 0.64 and 0.3, respectively (Table 8). Furthermore, the build-up of pressure likewise tends to sharp increase (by 30–40 kJ/mol) in the noted energy of activation of overall process and process of methane formation. As this takes place, the noted energies of activation approximate those for Co-containing catalysts of Fischer–Tropsch synthesis.

The build-up of pressure up to 20 atm is favourable for increasing selectivity of catalysts with respect to heavy hydrocarbons, however the selectivity relative to olefins is essentially reduced in the process to the level specific to selectivity of Co- and Fe-containing catalysts. A character of temperature dependence of selectivity relative to olefins is also changed. When a pressure is elevated to 10.4 atm, the selectivity relative to olefins is no longer temperature

TABLE 8

Results of catalytic tests of CoFeII-2 catalyst in Fischer–Tropsch synthesis at pressures of 1, 10.4 and 20.8 atm

Parameter	Pressure, atm				
	1			10.4	20.8
	at temperatures, °C				
	210	230	250	210	210
Speed of gas flow, $nL/(g_{cat} \cdot h)$	0.57	0.74	1.27	6.1	7.1
Degree of CO conversion, %	10.1	14.1	15.2	17.4	20.1
Rate of CO conversion, $mmol/(g_{cat} \cdot h)$	0.65	1.4	2.7	14.3	19.1
Frequency of CO conversion, $10^{-3}s^{-1}$	0.63	1.4	2.6	13.9	18.6
Noted E_{act} of CO conversion, kJ/mol	74			110	
Rate of CH_4 formation, $\mu mol/(g_{cat} \cdot h)$	60	148	295	1170	2970
Frequency of centre in reaction of CH_4 formation, $10^{-5}s^{-1}$	5.8	14.5	29	110	288
Selectivity in respect of methane, % C	9.2	11	11	8.2	15.6
Noted E_{act} of methanation, kJ/mol	84			150	
Selectivity in respect of CO_2, % C	23	28	30	3.9	4.4
α_{ASF} for *n*-paraffins C_{3-7}	0.71	0.69	0.68	0.70	0.61
α_{ASF} for *n*-paraffins C_{15+}				0.83	0.85
α_{ASF} for α-olefins C_{3-7}	0.32	0.29	0.26	0.21	0.28
α_{ASF} for α-olefins C_{15+}				0.64	0.66
C_3H_6/C_3H_8 ratio	6.0	6.9	10.2	3.3	1.9

Note. Characteristics of CoFeII-2: content of Me(I) + Me(II) is 21 mass %; particle size is 16 nm; number of surface centres Me^o is 0.28 $mmol/g_{cat}$.

dependent, whereas a rise in temperature at 20.8 atm causes the selectivity relative to olefins to decrease. The selectivity relative to CO_2 (CO vapour conversion route) is drastically reduced with increasing pressure and close to values characteristic of catalysts based on metallic cobalt.

The data of X-ray diffraction (see Fig. 3, curve *4*) point to the disruption of bimetallic structure under reaction conditions and the formation of individual phases of metallic iron ($d_{(110)}$ = 2.03 Å) and β-Co (reflexes at 2.05 and 1.77 Å) as well as to the availability of carbide phases (among them Co_2C: 2.11, 1.99, 1.62, and 1.58 Å) and a great quantity of carbon of graphite structure (d_{100} = 3.40 Å) in the catalyst. Consequently, the noted pronounced changes in properties of CoFeII-2 catalyst result from the change in the structure of catalytically active component in response to process conditions. By this means Co–Fe bimetallic phase identified in the catalyst and showing so superior selectivity relative to olefins is unstable and disrupted under Fischer–Tropsch synthesis conditions at elevated pressures. The study of the mechanism of bimetallic phase disruption in conditions of high partial pressure of synthesis gas and the possibility of this phase stabilization by adding, for one, promoters will be the theme of future investigations.

CONCLUSIONS

The results of pursued investigations allow following conclusions:

1. The deposition of binary complexes $[Ni(NH_3)_6]_3[Fe(CN)_6]_2$, $[Co(NH_3)_6][Fe(CN)_6]$ and $[Co(NH_3)_6]_2C_2O_4[Cu(C_2O_4)_2]_2$ on aluminium hydroxide and subsequent thermolysis of resultant composition are usable in the production of metallic particles (15–40 nm) fixed at the surface of aluminium oxide. In this case the use of binary complexes Ni–Fe and Co–Fe gives rise to bimetallic particles (15–16 nm) having respective fcc and bcc structures. For the examined Co–Cu ammonium oxalate complex, Cu^0 and cobalt carbide (Co_3C) phases rather than bimetallic particles are formed.

2. The disruption of complexes proceeds in several consecutive exothermic stages, and the partial decomposition of complexes $[Ni(NH_3)_6]_3[Fe(CN)_6]_2$ and $[Co(NH_3)_6]_2C_2O_4[Cu(C_2O_4)_2]_2$ takes place even at the stage of preparation and storage of initial composition of complex and aluminium hydroxide.

3. The metal/Al_2O_3 systems prepared by thermolysis of the studied compositions show catalytic activity in the reaction of CO hydrogenation. Ni–Fe bimetallic particles having FCC structure and Ni particles show similar properties in this reaction, but the first, as distinct from the second, are highly active in the reaction of CO vapour conversion, resulting in a high CO_2 content of the products. The catalytic properties of Fe–Co bimetallic particles having BBC structure prepared by thermolysis of $[Co(NH_3)_6][Fe(CN)_6]$ + $Al(OH)_3$ composition are much different from the properties of CoFe/TiO_2 catalysts described in the literature by reduced activity of these particles in respect to secondary processes of olefin hydrogenation. This characteristic manifests itself in the extremely high selectivity of the process in respect to olefins, among them ethylene, propylene, α-butene, and β-olefins C_{5+}, and in its anomalous temperature dependence. The origin of so low ability of the studied system to hydrogenate α-olefins remains to be explored and calls for further investigation.

4. The build-up of operating pressure to 10–20 atm tends to a marked change in catalytic properties, among them a decrease in selectivity relative to olefins and rate of secondary process of CO vapour conversion. The noted changes in catalytic properties result from the disruption of Fe–Co bimetallide having bcc structure in response to process conditions and the formation of phases of Co and Fe metallic particles as well as carbide structures and carbon of graphite structure.

REFERENCES

1 M. A. Vannice, *J. Catal.*, 37 (1975) 449.
2 P. J. Flory, *JACS*, 62 (1940) 1561.
3 R. A. Friedel, R. B. Anderson, *Ibid.*, 72 (1950) 2307.
4 M. A. Vannice, *J. Catal.*, 37 (1975) 449.
5 A. S. Lisitsyn, A. V. Golovin, V. L. Kuznetsov and Yu. I. Yermakov, *Ibid.*, 95 (1985) 527.
6 A. A. Khassin, T. M. Yurieva, V. N. Parmon, *Dokl. RAN*, 367, 3 (1999) 367.
7 D. J. Duvenhage, N. J. Coville, *Appl. Catal. A: Gen.*, 289 (2005) 231.
8 D. J. Duvenhage, N. J. Coville, *J. Mol. Catal. A: Chem.*, 235 (2005) 230.

9 S. I. Pechenyuk, D. P. Domonov, D. L. Rogachev, A. T. Belyaevskiy, *Zh. Neorg. Khim.*, 52, 7 (2007) 1110.
10 D. P. Domonov, S. I. Pechenyuk, N. L. Mikhailova, A. T. Belyaevskiy, *Ibid.*, 52, 7 (2007) 1104.
11 A. A. Khassin, Vliyaniye razmera chastits metallicheskikh Co i Ni na ikh kataliticheskiye svoystva v reaktsiyakh sinteza Fishera–Tropsha i disproportsionirovaniya CO (Candidate's Dissertation in Chemistry), Novosibirsk, 1998.
12 S. I. Pechenyuk, Yu. P. Semushin, D. P. Domonov *et al.*, *Koord. Khim.*, 31, 12 (2005) 912.
13 S. I. Pechenyuk, Yu. P. Semushin, D. P. Domonov, N. L. Mikhailova, *Ibid.*, 32, 8 (2006) 597.
14 G. Brower (Ed.), Inorganic Synthesis Guide [in Russian], Mir, Moscow, 1985, vol. 3.
15 Gmelins Handbuch der anorganischen Chemie. Kupfer, teil B, Lieferung 2, 1961, Verl. Chemie, Weinheim, S. 805.
16 B. K. Harned, C. J. Deere, *J. Biol. Chem.*, 104, 3 (1934) 727.
17 K. B. Arcuri, L. H. Schwartz, R. D. Pitrowski, J. B. Butt, *J. Catal.*, 85 (1984) 349.
18 D. J. Duvenhage, N. J. Coville, *Appl. Catal. A: Gen.*, 153 (1997) 43.
19 T. V. Reshetenko, L. B. Avdeeva, A. A. Khassin *et al.*, *Ibid.*, 268, 1–2 (2004) 127.
20 A. A. Khassin, T. M. Yurieva and V. N. Parmon, *React. Kinet. Catal. Lett.*, 64, 1 (1998) 55.
21 D. J. Duvenhage, N. J. Coville, *Appl. Catal. A: Gen.*, 289 (2005) 231.
22 D. J. Duvenhage, N. J. Coville, *J. Mol. Catal. A: Chem.*, 235 (2005) 230.
23 J. A. Amelse, L. H. Schwartz, J. B. Butt, *J. Catal.*, 72 (1981) 95.
24 L. M. Tau, H. Dabbagh, S. Bao and B. H. Davis, *Cat. Lett.*, 7 (1990) 127.
25 X. Zhan, H. J. Robota, K. B. Arcuri, Prepr. of ACS, *Div. Pet. Chem.*, 49, 2 (2004) 200.
26 T. K. Das, W. Conner, G. Jacobs, X. Zhan *et al.*, *Ibid.*, 49, 2 (2004) 161.